



Laminar smoke points of coflowing flames in microgravity

K.T. Dotson^a, P.B. Sunderland^{a,*}, Z.-G. Yuan^b, D.L. Urban^c

^a University of Maryland, Department of Fire Protection Engineering, 3104 J.M. Patterson Building, College Park, MD 20742, USA

^b National Center for Space Exploration Research, Cleveland, OH 44135, USA

^c NASA Glenn Research Center, Cleveland, OH 44135, USA

ARTICLE INFO

Article history:

Received 16 December 2010

Received in revised form

28 July 2011

Accepted 8 August 2011

Available online 1 September 2011

Keywords:

Combustion

Laminar gas jet diffusion flames

Residence time

Soot

ABSTRACT

Laminar smoke points were measured in nonbuoyant laminar jet diffusion flames in coflowing air. Microgravity was obtained on board the International Space Station. A total of 55 smoke points were found for ethylene, propane, propylene, and propylene/nitrogen mixtures. Burner diameters were 0.41, 0.76, and 1.6 mm, and coflow velocities varied from 5.4 to 65 cm/s. These flames allow extensive control over residence time via variations in dilution, burner diameter, and coflow velocity. The measured smoke-point lengths scaled with $d^{-0.91}u_{air}^{0.41}$, where d is burner diameter and u_{air} is coflow velocity. The measurements yielded estimates of sooting propensities of the present fuels in microgravity diffusion flames. Analytical models of residence times in gas jet flames are presented, and although residence time helps explain many of the observed trends it does not correlate the measured smoke points.

© 2011 Elsevier Ltd. All rights reserved.

1. Introduction

Soot is an important topic in fire and combustion research. Carbon monoxide is the major cause of death in fires and its emissions correlate with soot emissions. Radiation from soot contributes to increased fire spread rates and increased engine heat loads. The adverse health effects of soot exposure are significant [1] and soot is believed to contribute to climate change and glacial melting.

Laminar smoke points are the prevailing measure of fuel sooting tendency in diffusion flames. They are the conditions (and the luminous flame lengths) associated with incipient soot emission from diffusion flames. They have been measured in normal gravity for many gaseous, liquid, and solid [2,3] fuels and have aided the understanding of diverse flame systems. Smoke points correlate with important properties of turbulent diffusion flames, including soot volume fractions [4], radiative loss fractions [5,6], and soot emission rates [6–8]. They are important indicators of gas turbine soot emissions [6,9,10]. They are used increasingly in the development of numerical soot models for fire simulations [11–14].

There are four common explanations for the existence of smoke points, and these are not mutually exclusive. The first, and least controversial, is that smoke points occur when the soot temperature drops below a critical temperature prior to soot burnout. This temperature is about 1300 K in normal gravity

[15,16] and 1000 K in microgravity [17,18]. The second is that radiative loss fraction increases with fuel flow rate until it reaches 0.2–0.4 for normal-gravity smoke points [5,8,11,19,20] or 0.4–0.6 for microgravity smoke points [21]. The third explanation is that the ratio of luminous length divided by stoichiometric length increases with flow rate, and reaches about 2 at the smoke point [19,22,23], although no one has measured or modeled this ratio for microgravity flames at their smoke points. Unfortunately, these three explanations cannot be evaluated for the flames observed here because measurements of temperature, radiative loss fraction, and stoichiometric length were not possible. Flame residence time is the fourth common explanation and the most complex [7,15–18,21,22,24–27]. An increase in residence time can lead to soot emissions by increasing the time available for soot formation. Because this generally also increases the time available for soot oxidation, it has been proposed that smoke points are associated with conditions where the time available for soot formation exceeds that for soot oxidation [24]. Long residence times (accomplished, for example, by increasing burner diameter at a fixed fuel mass flow rate) can increase radiative loss fraction by decreasing scalar dissipation rates and increasing the volume of radiating soot and gas. Residence times in gas jet flames are afforded the most control when tests are performed in microgravity with a controllable coflow, which is the method adopted here.

Sunderland et al. [24] reported the first microgravity smoke points, which were on board a microgravity aircraft. Microgravity smoke-point measurements are difficult in both aircraft (owing to g-jitter) and in drop facilities (owing to limited test times). Recognizing this, Urban et al. [21] reported smoke points in earth

* Corresponding author. Tel.: +1 301 405 3095; fax: +1 301 405 9383.
E-mail address: pbs@umd.edu (P.B. Sunderland).

Nomenclature

a	constant in Eq. (7)
A_f	constant in Eq. (7)
b	constant in Eq. (7)
B	constant in Eq. (3)
C	constant in Eq. (2)
d	burner inside diameter
g	acceleration due to gravity
i	species index
L	luminous flame length
\dot{m}_f	fuel mixture mass flow rate
R^2	coefficient of determination
Re	burner Reynolds number, $u_f d/\nu_f$
T_{ad}	adiabatic flame temperature
t_{res}	centerline residence time, Eq. (1)
u	axial velocity
X	mole fraction
Y	mass fraction

z	axial distance
Z_{st}	stoichiometric mixture fraction

Greek symbols

ν	kinematic viscosity
ρ	density

Subscripts

0	virtual origin
1g	normal gravity
air	coflowing air
cl	centerline
f	fuel or fuel/inert mixture
mix	mixture
SP	smoke point

orbit, considering ethylene and propane in quiescent air. The present study extends this past work to microgravity smoke points in coflowing air.

Microgravity smoke points are of interest to spacecraft fire safety. Microgravity allows improved control over residence time and can improve the understanding of the different mechanisms responsible for smoke points in normal gravity and microgravity [17–19,21,24]. In particular, accelerating flows in normal gravity reduce the time available for soot oxidation, whereas decelerating flows in microgravity can lead to radiative quenching of soot reactions [21,24]. Different entrainment behavior also contributes to different smoke-point behavior in normal gravity and in microgravity [21,24].

The effects of coflow on soot processes can be complex, as coflow can modify entrainment, temperature, and residence time. Increased coflow velocity can either increase or decrease soot concentrations. A 2.5 s drop tower study by Jeon et al. [28] found that soot concentration increased with coflow velocity. This was attributed to increased temperatures, but transient effects may also have contributed. Faeth and co-workers [25,26,29] studied weakly buoyant flames and found that increased coflow velocity reduced soot concentrations and increased smoke-point lengths. This was attributed to decreased flame residence time and modified entrainment. In contrast, Sivathanu and Faeth [7] found that smoke points decreased with increasing coflow velocity.

Much remains unknown about the effects of gravity and coflow velocity on smoke points. Thus, the objectives of this study are to measure laminar smoke points of coflowing gas jet flames in long-duration microgravity; to quantify the effects of burner diameter, coflow velocity, and residence time on the smoke points; and to determine microgravity sooting propensities of various fuels and diluted fuels.

2. Residence time analysis

Given the importance of flow time for soot processes [7,15–18,21,22,24–27], residence time is considered here analytically. Centerline residence time for steady laminar gas jet flames is defined as

$$t_{res} = \int_0^L u_{cl}^{-1} dz. \quad (1)$$

This relationship can be exploited by invoking the flame length scaling for both luminous and stoichiometric lengths of steady laminar gas jet diffusion flames of

$$L = C\dot{m}_f / (\rho\nu_{air}), \quad (2)$$

where C is a dimensionless constant that depends on the fuel and the oxidizer, but is essentially independent of burner diameter, pressure, gravity level, and coflow velocity [19,21,25,26,29–31].

Eqs. (1) and (2) yield simple scaling laws for three limiting cases: strongly buoyant flames, nonbuoyant flames with matched velocity coflow, and nonbuoyant flames with quiescent ambient. For strongly buoyant flames, $u_{cl} \sim (gz)^{1/2}$, where \sim denotes proportionality [11,14,16,32]. Combining this with Eqs. (1) and (2) yields $t_{res} \sim (L/g)^{1/2}$ [16,22]. For nonbuoyant flames with matched velocity coflow, u_{cl} is approximately constant and equal to u_f . Combining this with Eqs. (1) and (2) yields $t_{res} \sim d^2/\nu_{air}$. For nonbuoyant flames with quiescent ambient, Spalding [33] obtained the velocity scaling of $u_{cl} \sim (u_f d)^2 / (\nu_{air} z)$. When combined with Eqs. (1) and (2), this also yields $t_{res} \sim d^2/\nu_{air}$. These scaling laws are summarized in Table 1. An increase in fuel flow rate for buoyant flames increases residence time, but has no effect on residence time for both types of nonbuoyant flames. This once led to the prediction that smoke points would not exist for nonbuoyant gas jet flames [16].

While these simple scaling laws yield insight, they cannot explain all aspects of smoke-point behavior and they do not correlate smoke points [27]. For example, microgravity smoke points in still air are observed to have little dependence on burner diameter [21,24], but for these flames $t_{res} \sim d^2/\nu_{air}$. Thus, a more complex model of residence time is developed below.

Table 1

Summary of scaling laws for centerline velocity and residence time for several assumed gas jet conditions^a.

Condition	u_{cl}	t_{res}
Strongly buoyant	$(gz)^{1/2}$	$(L/g)^{1/2}$
Nonbuoyant with matched velocity coflow	u_f	d^2/ν_{air}
Nonbuoyant with quiescent ambient	$(u_f d)^2 / (\nu_{air} z)$	d^2/ν_{air}

^a Assuming $L = C\dot{m}_f / (\rho\nu_{air})$ and a virtual origin coincident with the burner. The relationships shown are valid for variations in d , fuel flow rate, and pressure.

There are no known similarity solutions of the momentum equation for coflowing jets. However, the Spalding [33] similarity solution was extended by Lee et al. [34] to approximately incorporate the effects of coflowing oxidizer using superposition. Lee et al. [34] found their analytical velocities agreed with experiments when $u_f \gg 2u_{air}$. Note that $u_f > 2u_{air}$ for 61% of the present smoke points. Lee et al. [34] found the following relation for centerline velocity when the initial fuel velocity profile is Pouiselle:

$$u_{cl} = u_{air} + B/(z - z_0), \quad (3)$$

where

$$B = \frac{(du_f)^2}{\nu_{air}} \left(\frac{\rho_f}{8\rho_{air}} - \frac{3u_{air}}{32u_f} \right). \quad (4)$$

In Eq. (4), ρ_f is the fuel mixture density at 294 K and ν_{air} is air viscosity at 1500 K [35], i.e., $2.291 \times 10^{-4} \text{ m}^2/\text{s}$. The virtual origin of Lee et al. [34] is simplified here to the following, chosen such that the centerline velocity of Eq. (3) matches the centerline velocity at the burner discharge and at infinite axial distance:

$$z_0 = B/(u_{air} - 2u_f) \quad (5)$$

While it is possible for the virtual origin to become positive [29], leading to a singularity in the velocity field of Eq. (3), this does not occur for the present flames.

Inserting Eq. (3) into Eq. (1) and integrating yields the following centerline residence time for coflowing flames in microgravity:

$$t_{res} = \frac{z}{u_{air}} - \frac{B}{u_{air}^2} \ln \left| 1 + \frac{zu_{air}(2u_f - u_{air})}{2Bu_f} \right|. \quad (6)$$

Inserting $z = L_{SP}$ then yields the smoke-point centerline residence time.

Eq. (6) indicates that residence time increases with fuel flow rate when coflow velocity is small, but decreases with fuel flow rate when coflow velocity is large. This suggests the possible existence at high coflow velocity of inverse smoke points – laminar flames that emit soot at low fuel flow rates, but not at high flow rates. Inverse smoke points were not observed here even though many tests involved large coflow velocities.

3. Experimental methods

The Smoke Point in Coflow Experiment (SPICE) was operated in the Microgravity Science Glovebox on board the International Space Station (ISS) in 2009. The fuels considered are shown in Table 2. Smoke points were attempted with methane, but could not be obtained before the flames impinged on the downstream copper plate. Burner diameters were 0.41, 0.76, and 1.60 mm.

Table 2
Summary of the observed coflowing microgravity smoke points^a.

Parameter	C ₂ H ₄	C ₃ H ₈	C ₃ H ₆	75% C ₃ H ₆	50% C ₃ H ₆
Z_{st}	0.0637	0.0603	0.0637	0.0768	0.1018
T_{ad} , K	2367	2264	2332	2317	2288
u_f , cm/s	69.6–735	48.9–460	11.2–764	19.5–274	49.6–113
\dot{m}_f , mg/s	1.63–3.89	1.80–3.84	0.39–1.73	0.63–2.00	1.45–3.29
Re	127–636	176–788	36.4–630	47.4–317	90.7–207
No. of smoke points	6	6	22	14	7
A_f , mm	21.2	18.5	6.05	7.65	13.9
$L_{SP,1g}^b$, mm	106	162	29	35.4	48.3

^a All flames were attached to the burner, i.e., not lifted. For mixtures, the fuel mole fraction is shown and the inert is N₂. Parameters u_f and Re assume conditions of 294 K, 1.01 bar, uniform velocity, and fuel mixture viscosity.

^b Normal-gravity smoke points are from Schug et al. [30]. For propylene/nitrogen mixtures, these are estimated using the propylene smoke point of 29 mm and Eq. (9).

The SPICE module contained a rectangular duct with a 76 × 76 mm square cross section with rounded corners. A DC fan supplied coflowing air from the Glovebox contents. The air passed through a honeycomb and inlet screen to reduce swirl and then entered the duct. The air and combustion products left the duct through a perforated copper plate followed by a brass screen. The inlet screen was 50 mm upstream of the jet exit, and the copper plate was 120 mm downstream. Fan voltage was varied to control the coflow velocity, which was measured with a hot-sphere anemometer located between the inlet honeycomb and screen. This anemometer was calibrated in normal gravity using a transfer standard of a calibrated hot-wire anemometer placed at the centerline 13 mm downstream of the jet exit. Velocities at other locations in the flow duct were found to be within ± 10% of the velocity at this location. Additional details of the experimental hardware, including images, are given by Dotson [36].

Fuel flow rate was adjusted manually and controlled with a mass flow meter. The flames were ignited with a hot-wire igniter. Video was recorded with an analog color video camera and downlinked in real time. Still images were recorded with a 12 bit Nikon™ D100 color camera (3008 × 2000 pixels) with a 60 mm lens. Additional details are given by Dotson [36].

Most tests were conducted by setting the coflow velocity, igniting the flame, and manually adjusting the fuel flow rate to seek out and traverse the smoke points. Approximate smoke points were identified in the video by the flight crew and simultaneously by the ground support team in Cleveland. Typical burn times were 60 s and after each burn the glovebox was flushed with cabin air. The oxygen mole fraction of ISS cabin air was maintained within an estimated range of 20–23%.

The video record was analyzed after the tests to more precisely identify smoke points. The smoke-point lengths were measured from the burner to the tip of the luminous flame on its axis. The luminous flame tips were not sharply defined in most flames, but instead transitioned from bright yellow to black over an axial distance of 2–5 mm. Luminous lengths were measured to the point where the centerline grayscale intensity changed most rapidly between these yellow and black regions. This helped reduce the sensitivity of the measured lengths to camera exposures.

Uncertainties in the measurements are estimated at ± 5% for fuel velocity, ± 10% for air velocity, and ± 5% for luminous length. Repeatability of the smoke-point lengths is estimated at ± 5%, except for tests using the 0.41 mm burner, which had an estimated repeatability of ± 10%.

4. Results and discussion

The flames generally reached steady conditions within 10 s of ignition, or within 5 s of a change in fuel or air flow rate. Flames of

propylene and propylene mixtures were generally more luminous than the others, attributed to increased soot volume fractions. Periodic flame motion was observed in some flames, especially those with high air velocity, large burners, and long flames, and is attributed to unsteady coflow. This slightly increased the uncertainties in smoke points for these conditions.

The conditions for which smoke points were found are summarized in Table 2. In some cases, e.g., tests involving ethylene, the fuel supply was depleted before all desired conditions could be tested, as the supply was limited to two 150 cc bottles of each fuel at gage pressures of 760–1440 kPa.

Smoke points for propane and ethylene were generally identified by the onset of gradual dimming, reddening, and rounding of the luminous flame tip. The brightest flames, generally for propylene and propylene mixtures, normally did not display significant dimming and reddening near their tips except when much longer than their smoke points. Smoke points for these flames were identified by the rapid transition to open-tipped flames. Open-tipped flames are common in both normal gravity and microgravity when smoke points are far exceeded [21] and are generally associated with local flame extinguishment along the centerline and soot emission in an annular shell. For conditions sufficiently above the smoke points a glowing stream of particles could be seen leaving the flame.

Fig. 1 shows color images from the still camera for representative flames near their smoke points. Two sequences are shown, and in both the smoke point occurs between the third and fourth images. In the top row coflow velocity decreases from left to right at a constant fuel flow rate. This increases luminous flame length and leads to open-tipped soot emission in the fourth image. The luminous length decreases in the fourth image owing to flame extinction and reactant leakage. In the bottom row fuel flow rate is increased at a constant coflow velocity, thus increasing luminous lengths. The luminous lengths of the flames in Fig. 1 are more sensitive to changes in fuel flow rate than to changes in coflow velocity.

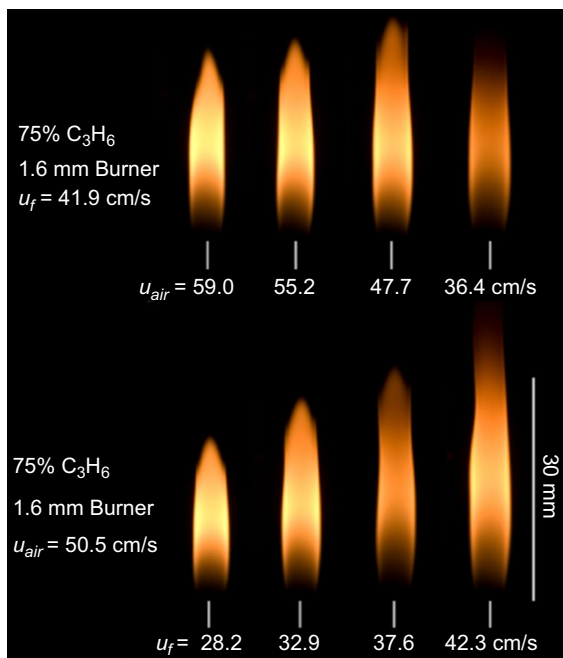


Fig. 1. Still camera images of 75% C₃H₆ microgravity flames with 1.6 mm burner and with (top) decreasing coflow velocity and (bottom) increasing fuel flow rate. Short vertical lines show the burner position. Images were taken at *f*/11 with a shutter speed of 3.1 ms, except the rightmost image in the top row and third image in the bottom row, which used a shutter speed of 1.3 ms. Original in color.

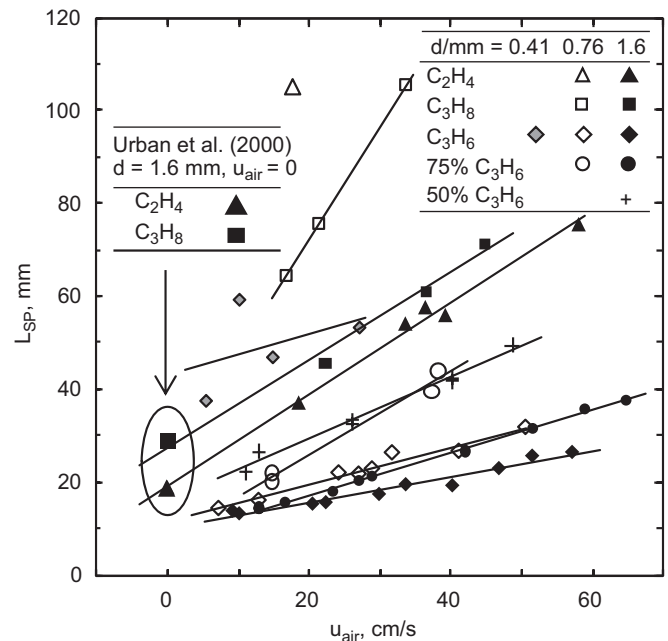


Fig. 2. Microgravity smoke point luminous length plotted with respect to coflow velocity. The lines shown are fits for each pairing of fuel and burner diameter. Quiescent data from Urban et al. [21] at 1.01 bar are included in two of the fits.

Measured microgravity smoke points are plotted in Fig. 2 with respect to coflow velocity for the present coflowing flames. Also shown are two flames in quiescent ambient from Urban et al. [21], which agree with the trends in coflow velocity established by the coflowing tests. Smoke-point lengths in coflow generally increase with decreasing burner diameter and, in agreement with normal-gravity results [25,26,36], with increasing coflow velocity. This is expected because a decrease in burner diameter – or an increase in coflow velocity – decreases the residence time available for soot formation and decreases radiative loss fraction by increasing scalar dissipation rates and by making the flame shorter and narrower.

It is unknown why the effect of burner diameter diminishes with the approach to quiescent ambients. This behavior agrees with observations of nonbuoyant noncoflowing flames [21] and normal-gravity flames in weak coflow [21,24].

An analysis of the coflow flame measurements of Fig. 2 was undertaken to quantify the dependence of smoke points on burner diameter, coflow velocity, and fuel. Correlations were sought in the form of

$$L_{SP} = A_f d^a u_{air}^b, \quad (7)$$

where *d* is in mm, *u_{air}* is in cm/s, *a* and *b* are constants, and *A_f* is a constant for each fuel mixture. Constants *a*, *b*, and *A_f* were found from the measurements such that the *R*² coefficient of determination between the two sides of Eq. (7) was maximized and the fit slope was unity for the present coflow smoke points. The results were *a* = −0.910, *b* = 0.414, and *A_f* values as shown in Table 2. The associated plot is shown in Fig. 3. The measurements are reasonably well correlated across a broad range of fuel sooting propensities, smoke-point lengths, burner diameters, and coflow velocities. The correlation indicates a scaling for the present smoke points of $L_{SP} \sim d^{-0.91} u_{air}^{0.41}$. The negative and positive exponents on *d* and *u_{air}*, respectively, are consistent with the above discussion of Fig. 2. This scaling does not apply for quiescent ambients, for which smoke heights of zero would be predicted. Although the microgravity data of Urban et al. [21] are plotted in Fig. 3, they were not included in the correlation.

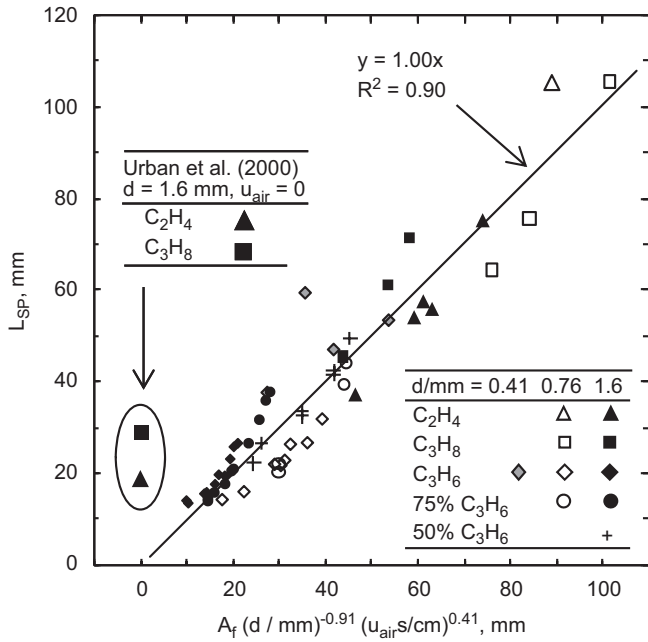


Fig. 3. Correlation of microgravity smoke points with A_f , d and u_{air} . Data for Urban et al. [21] at 1.01 bar are not included in the fit. Values of A_f are shown in Table 2.

Quantity A_f is proportional to a nominal laminar smoke point, e.g., for different fuels at a fixed d and u_{air} . It indicates the following sooting propensity ranking for the present fuels in coflowing microgravity flames:

ethylene < propane < 50% propylene < 75% propylene < propylene. (8)

Excepting ethylene and propane, these trends are readily evident in Fig. 2. The only surprise of this ranking is that propane soots more than ethylene, which has not been observed in previous normal-gravity [7,30] or microgravity tests [21,24].

The normal-gravity smoke points of Schug et al. [30] for ethylene, propane, and propylene burning on a 10 mm burner are given in Table 2. The normal-gravity smoke points of the propylene mixtures are estimated as follows. Gill and Olson [37] proposed a mixing relationship for fuel mixtures, also used by others [10,38], that simplifies to

$$\frac{1}{L_{SP,mix}} = \sum_i \frac{Y_i}{L_{SP,i}} \quad (9)$$

Markstein [20] proposed the similar form of

$$\frac{1}{L_{SP,mix}} = \sum_i \frac{X_i}{L_{SP,i}} \quad (10)$$

where Eq. (10) assumes proportionality between luminous flame length and fuel flow rate. Although Eqs. (9) and (10) were developed for mixtures of pure fuels, it is assumed here that these equations also apply for fuel/inert mixtures [30,39] when the inert is assigned an infinite smoke-point length. Eq. (9) allowed the normal-gravity smoke points for propylene/nitrogen mixtures to be estimated in Table 2. The result is the following sooting propensity ranking in normal gravity:

propane < ethylene < 50% propylene < 75% propylene < propylene. (11)

This agrees with the microgravity ranking, Eq. (8), except for the exchanged positions of propane and ethylene.

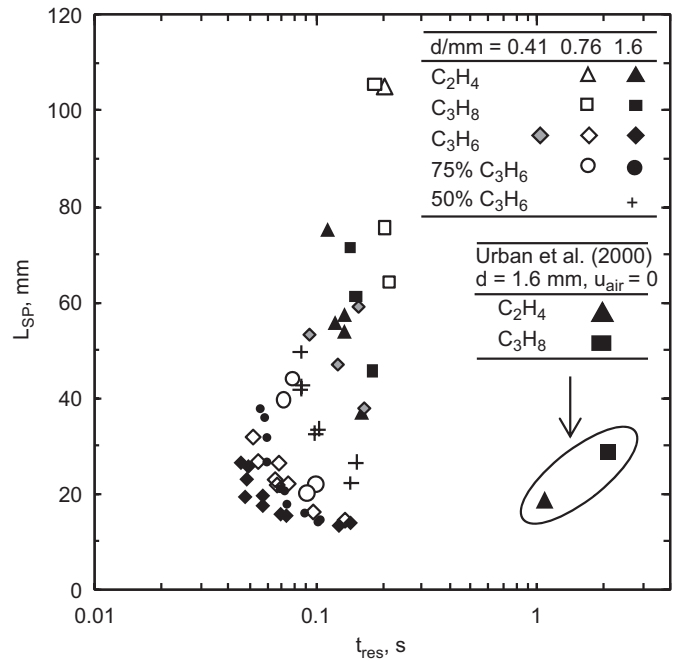


Fig. 4. Microgravity smoke point versus centerline residence time as predicted by Eq. (6).

The microgravity smoke points for propane are shorter than for ethylene for the 0.76 mm burner, leading to propane's lower value of A_f . Note that this is not the case for the 1.6 mm burner. Propane's increased molecular weight relative to ethylene's yields a lower initial fuel velocity for the same luminous flame length. In microgravity (but less so in normal gravity) this lower velocity increases the time available for soot formation, thus increasing sooting propensity. This effect is not seen for propylene, probably because its smoke points are shorter and thus less affected by changes in gravity level.

Owing to extensive past use of residence time to explain smoke-point behavior, Fig. 4 is a plot of total flame residence time, from Eq. (6) with $z=L_{SP}$, versus smoke-point length for the present flames and those of Urban et al. [21]. Extensive scatter in this plot confirms past findings that microgravity smoke points do not have constant residence times [21]. For a given fuel mixture and burner diameter, residence time generally decreases with increasing smoke-point length (achieved here by increasing u_{air}). Note that the residence times for propane, propylene, and 75% propylene with the 1.6 mm burner generally involve $u_f < 2u_{air}$, and thus are less accurate. Plots were also made with the abscissa of Fig. 4 changed to soot formation time, soot oxidation time, and formation/oxidation time, but none yielded a successful correlation with smoke point. For these, the transition between soot formation and oxidation was assumed to occur at $z=L_{SP}/2$ [19,22,23].

5. Conclusions

Smoke points of 55 microgravity gas jet diffusion flames in coflowing air were measured in earth orbit. The conditions emphasized small burners and the effects of coflow velocity. These flames allow extensive control over residence time. The major conclusions are as follows:

1. The present smoke-point lengths scale with $d^{-0.91} u_{air}^{0.41}$. Either a decrease in diameter or an increase in coflow velocity

decreases residence time and radiative loss fraction, which in turn leads to a longer smoke point.

- The sooting propensities of the present fuel mixtures in microgravity increase according to ethylene < propane < 50% propylene < 75% propylene < propylene. This is the same as in normal gravity except for the exchanged positions of ethylene and propane.
- Several scaling laws for residence time in gas jet flames are presented, including one for coflowing microgravity flames. Although residence time is helpful in understanding the present smoke points, it does not yield quantitative correlations.

Acknowledgments

Work at the University of Maryland was supported by NASA cooperative agreement NNX07-AO91A and the Department of Fire Protection Engineering. The authors acknowledge G.M. Faeth for conceiving this work, M.A. Delichatsios for help with residence times, the SPICE engineering team for building the hardware, and astronauts M. Barratt, E.M. Fincke, S.H. Magnus, and K. Wakata for conducting the tests.

References

- I.M. Kennedy, The health effects of combustion-generated aerosols, *Proc. Combust. Inst.* 31 (2007) 2757–2770.
- G.T. Linteris, I.P. Rafferty, Flame size, heat release, and smoke points in materials flammability, *Fire Saf. J.* 43 (2008) 442–450.
- K.M. Allan, J.R. Kaminski, J.C. Bertrand, J. Head, P.B. Sunderland, Laminar smoke points of wax candles, *Combust. Sci. Technol.* 181 (2009) 800–811.
- J.H. Kent, Turbulent diffusion flame sooting – relationship to smoke-point tests, *Combust. Flame* 67 (1987) 223–233.
- G.H. Markstein, Relationship between smoke point and radiant emission from buoyant turbulent and laminar diffusion flames, *Proc. Combust. Inst.* 20 (1984) 1055–1061.
- Y. Yang, A.L. Boehman, R.J. Santoro, A study of jet fuel sooting tendency using the threshold sooting index (TSI) model, *Combust. Flame* 149 (2007) 191–205.
- Y.R. Sivathanu, G.M. Faeth, Soot volume fractions in the overfire region of turbulent-diffusion flames, *Combust. Flame* 81 (1990) 133–149.
- M.A. Delichatsios, Smoke yields from turbulent buoyant jet flames, *Fire Saf. J.* 20 (4) (1993) 299–311.
- N.D. Marsh, I. Preciado, E.G. Eddings, A.F. Sarofim, A.B. Palotas, J.D. Robertson, Evaluation of organometallic fuel additives for soot suppression, *Combust. Sci. Technol.* 179 (2007) 987–1001.
- A. Mensch, R.J. Santoro, T.A. Litzinger, S.-Y. Lee, Sooting characteristics of surrogates for jet fuels, *Combust. Flame* 157 (2010) 1097–1105.
- M.A. Delichatsios, A phenomenological model for smoke-point and soot formation in laminar flames, *Combust. Sci. Technol.* 100 (1994) 283–298.
- C.W. Lautenberger, J.L. de Ris, N.A. Dembsey, J.R. Barnett, H.R. Baum, A simplified model for soot formation and oxidation in CFD simulation of non-premixed hydrocarbon flames, *AIAA J.* 40 (2005) 141–176.
- T. Beji, J.P. Zhang, M. Delichatsios, Determination of soot formation rate from laminar smoke point measurements, *Combust. Sci. Technol.* 180 (2008) 927–940.
- T. Beji, J. Zhang, M. Delichatsios, Soot formation and oxidation in fires from laminar smoke point measurements, *Proc. Int. Symp. Fire Saf. Sci.* 9 (2008) 219–230.
- J.H. Kent, H.G. Wagner, Why do diffusion flames emit smoke? *Combust. Sci. Technol.* 41 (1984) 245–269.
- I. Glassman, Soot formation in combustion processes, *Proc. Combust. Inst.* 22 (1988) 295–311.
- D.L. Urban, Z.-G. Yuan, P.B. Sunderland, G.T. Linteris, J.E. Voss, K.-C. Lin, Z. Dai, K. Sun, G.M. Faeth, Structure and soot properties of nonbuoyant ethylene/air laminar jet diffusion flames, *AIAA J.* 36 (8) (1998) 1346–1360.
- G.M. Faeth, in: H.D. Ross (Ed.), *Microgravity Combustion: Fire in Freefall*, Combustion Treatise, Academic Press, San Diego, CA, USA, 2001, p. 83.
- F.G. Roper, C. Smith, Soot escape from laminar air-starved hydrocarbon flames, *Combust. Flame* 36 (1979) 125–138.
- G.H. Markstein, Radiant emission and smoke points for laminar diffusion flames of fuel mixtures, *Proc. Combust. Inst.* 21 (1986) 1107–1114.
- D.L. Urban, Z.-G. Yuan, P.B. Sunderland, K.-C. Lin, Z. Dai, G.M. Faeth, Smoke-point properties of nonbuoyant round laminar jet diffusion flames, *Proc. Combust. Inst.* 28 (2000) 1965–1972.
- F.G. Roper, Soot escape from diffusion flames: a comparison of recent work in this field, *Combust. Sci. Technol.* 40 (1984) 323–329.
- K.-C. Lin, G.M. Faeth, P.B. Sunderland, D.L. Urban, Z.-G. Yuan, Shapes of nonbuoyant round luminous hydrocarbon/air laminar jet diffusion flames, *Combust. Flame* 116 (1999) 415–431.
- P.B. Sunderland, S. Mortazavi, G.M. Faeth, D.L. Urban, Laminar smoke points of nonbuoyant jet diffusion flames, *Combust. Flame* 96 (1994) 97–103.
- K.-C. Lin, G.M. Faeth, Hydrodynamic suppression of soot emissions in laminar diffusion flames, *J. Propul. Power* 12 (1) (1996) 10–17.
- Z. Dai, G.M. Faeth, Hydrodynamic suppression of soot formation in laminar coflowing jet diffusion flames, *Proc. Combust. Inst.* 28 (2000) 2085–2092.
- T.L. Berry, W.L. Roberts, Measurement of smoke point in velocity-matched coflow laminar diffusion flames with pure fuels at elevated pressures, *Combust. Flame* 145 (2006) 571–578.
- B.-H. Jeon, O. Fujita, Y. Nakamura, H. Ito, Effect of co-axial flow velocity on soot formation in a laminar jet diffusion flame under microgravity, *J. Therm. Sci. Technol.* 2 (2) (2007) 281–290.
- K.-C. Lin, G.M. Faeth, Shapes of nonbuoyant round luminous laminar-jet diffusion flames in coflowing air, *AIAA J.* 37 (6) (1999) 759–765.
- K.P. Schug, Y. Manheimer-Timnat, P. Yaccarino, I. Glassman, Sooting behavior of gaseous hydrocarbon diffusion flames and the influence of additives, *Combust. Sci. Technol.* 22 (1980) 235–250.
- P.B. Sunderland, B.J. Mendelson, Z.-G. Yuan, D.L. Urban, Shapes of buoyant and nonbuoyant laminar jet diffusion flames, *Combust. Flame* 116 (1999) 376–386.
- F.G. Roper, The prediction of laminar jet diffusion flame sizes: part 1. theoretical model, *Combust. Flame* 29 (1977) 219–226.
- D.B. Spalding, *Combustion and Mass Transfer*, Pergamon, New York, 1979 p. 185.
- J. Lee, S.H. Won, S.H. Jin, S.H. Chung, Lifted flames in laminar jets of propane in coflow air, *Combust. Flame* 135 (2003) 449–462.
- F.G. Roper, C. Smith, A.C. Cunningham, The prediction of laminar jet diffusion flame sizes: part II. experimental validation, *Combust. Flame* 29 (1977) 227–234.
- K.T. Dotson, Smoke Points of Microgravity and Normal Gravity Coflow Diffusion Flames, M.S. Thesis, University of Maryland, College Park, USA, <<http://drum.lib.umd.edu/>>, 2009, 82 pp.
- R.J. Gill, D.B. Olson, Estimation of soot thresholds for fuel mixtures, *Combust. Sci. Technol.* 40 (1984) 307–315.
- P. Pepiot-Desjardins, H. Pitsch, R. Malhotra, S.R. Kirby, A.L. Boehman, Structural group analysis for soot reduction tendency of oxygenated fuels, *Combust. Flame* 154 (2008) 191–205.
- T.L. Berry, W.L. Roberts, Effect of dilution, pressure, and velocity on smoke point in laminar jet flames, *Combust. Sci. Technol.* 180 (2008) 1334–1346.